EUROFUSION WPSA-PR(16) 16483

A. Mele et al.

Control-oriented tools for the design and validation of the JT-60SA magnetic control system

Preprint of Paper to be submitted for publication in
Control Engineering Practice

This work has been carried out within the framework of the EUROfusion Consortium and has received funding from the Euratom research and training programme 2014-2018 under grant agreement No 633053. The views and opinions expressed herein do not necessarily reflect those of the European Commission.

Control-oriented tools for the design and validation of the JT-60SA magnetic control system

N. Cruz[a], G. De Tommasi[b,d], M. Mattei[c,d], A. Mele[b,d], Y. Miyata[e], A. Pironti[b,d], T. Suzuki[e]

[a]*Instituto de Plasmas e Fusão Nuclear, Instituto Superior Técnico, Universidade de Lisboa, 1049-001 Lisboa, Portugal*
[b]*Dipartimento di Ingegneria Elettrica e delle Tecnologie dell'Informazione, Università degli Studi di Napoli Federico II, via Claudio 21, 80125, Napoli, Italy*
[c]*Dipartimento di Ingegneria Industriale e dell'Informazione, Seconda Università degli Studi di Napoli, via Roma 29, Aversa (CE), 80131, Italy*
[d]*Consorzio CREATE, via Claudio 21, 80125, Napoli, Italy*
[e]*National Institutes for Quantum and Radiological Science and Technology, Naka, Ibaraki, 311-0193, Japan*

Abstract

The construction and operation of the JT-60SA tokamak is the main project currently carried out jointly by Japan and the European Union under the Broader Approach agreement. Within the Integrated Project Team, Japanese and European scientists are developing and testing a number of tools to support preliminary studies and future operations of JT-60SA. Within this collaborative framework, European scientists are using a set of assessed modeling tools to design and validate possible solutions for the plasma magnetic control system of JT-60SA.

This paper introduces these tools and describes a possible control architecture to be used on the JT-60SA tokamak. The effectiveness of the proposed architecture is shown by means of numerical simulations.

Keywords: JT-60SA; Control in fusion devices; Plasma magnetic control in tokamak.

Email addresses: nunocruz@lei.fis.uc.pt (N. Cruz), detommas@unina.it (G. De Tommasi), massimiliano.mattei@unina2.it (M. Mattei), adriano.mele@unina.it (A. Mele), miyata.yoshiaki@qst.go.jp (Y. Miyata), pironti@unina.it (A. Pironti), suzuki.takahiro@qst.go.jp (T. Suzuki)

1. INTRODUCTION

The Broader Approach (BA) is an agreement between the European Union and Japan that complements the ITER Project. BA aims to accelerate the realisation of fusion energy by carrying out R&D, and by developing some advanced technologies for future demonstration fusion power reactors [29].

The Satellite Tokamak Programme (STP) is the main project within the BA umbrella; it includes the construction of the JT-60SA superconductive tokamak and its exploitation as an ITER "satellite" facility [31, 28]. The STP is expected to develop operating scenarios and address key physics issues for an efficient start up of ITER and for providing a continuous support to ITER experimentation. Furthermore it is expected that the operation of JT-60SA will complement the one of ITER in all areas of fusion R&D which are necessary to proceed with the design and realization of DEMO [20].

The European contribution to the STP programme is significant and it is not limited to the tokamak construction. Indeed, European scientists are actively contributing to the definition of the JT-60SA research plan [18], and it is planned that the European team will be actively involved in the operations, playing a relevant role. For this reason, preliminary studies related to the exploitation of JT-60SA are currently carried out in different fields by European scientists in collaboration with Japanese colleagues.

Furthermore, the European Union aims at participating not only to the physics exploitation, but also at giving engineering support during the operations ([18, 19]).

In this context the European fusion community is developing a number of tools for the design and validation of control systems, especially for magnetic axisymmetric control [9, 14].

Axisymmetric magnetic control deals with the control of the external magnetic field in a tokamak, which is necessary to achieve and maintain the desired *operational scenario*, that includes the desired current, and the desired shape and position of the plasma column within the vacuum chamber. On top of that, in all modern high performance tokamaks, due to the elongated and vertically unstable plasmas, magnetic control is also mandatory in order to achieve stable plasmas. Moreover, for energetic reasons, the plasma should occupy as much volume as possible; this means that the distance between the plasma boundary and the facing metallic structures should be kept small and should be robustly controlled. To sum up, magnetic control represents the basic feedback control system that is

needed in a tokamak since early operation phases, including the commissioning of the power supplies for the Poloidal Field (PF) coils, since magnetic control usually includes also the regulation of the current in the PF circuits [26, 33].

Within the European fusion community, the CREATE team has gained a significant experience in developing tools for the design and validation of magnetic control systems. The tools developed by CREATE have been validated on a number of different experimental devices (among the various see [30, 3, 10]), and have been successfully used to design magnetic control systems, for example at TCV [7] and JET [5, 15, 16]. Furthermore, these tools are currently used to propose an enhancement of the EAST plasma control system [2], and to perform preliminary studies and code benchmarking for both ITER [34, 22, 6] and DEMO [32].

Within the dedicated workpackage of the Eurofusion activities, the CREATE tools are currently exploited to perform preliminary studies on the plasma magnetic control of JT-60SA. In particular, this paper reports on a possible architecture for this control system that has been designed and validated in simulation by exploiting the CREATE modeling codes.

It should be noticed that the equilibrium codes presented in this paper can be effectively used also to benchmark the scenarios studies made by the Japanese scientists [21]; an example of comparison between equilibria is given in this paper.

The paper is structured as follows: Section 2 gives a description of the JT-60SA PF coils system and introduces to the main axisymmetric magnetic control problems. Section 3 describes the tools that have been developed to design and validate magnetic control systems. A possible architecture for the magnetic control system of JT-60SA is proposed in Section 4, while some preliminary simulation results obtained using the proposed tools are presented in Section 5. Eventually, some conclusive remarks are given.

2. MAGNETIC CONTROL IN JT-60SA

In this section, first a brief description of the main characteristics of the JT-60SA tokamak and, in particular, of its PF coils is given; these coils, indeed, represent the actuators used by any magnetic control system. In the second part, the reader is introduced to the main axisymmetric magnetic control problems, i.e. plasma current, position and shape control.

2.1. The JT-60SA PF coils system

The JT-60SA tokamak is currently under construction in Naka, in the Ibaraki Prefecture of Japan, as a part of STP. The plasma in the JT-60SA vacuum chamber, will have a major radius of $2.96\ m$ and a minor radius of $1.18\ m$, with an overall plasma volume of $132\ m^3$ [31]. The maximum plasma current envisaged for JT-60SA is $5.5\ MA$ for a plasma with a relatively low aspect ratio (elongation $\kappa = 1.93$ and triangularity $\delta = 0.53$), and $4.6\ MA$ for an *ITER-shaped* plasma ($\kappa = 1.8$ and $\delta = 0.43$). The maximum pulse duration will be about $100\ s$ [20].

After the machine upgrade, JT-60SA will have a PF coils system consisting of two sets of superconductive coils: the Equilibrium Field Coils (*EF1-6*) made of Niobium-Titanium ($NbTi$), and the Central Solenoid (consisting of four independent coils, named *CS1-4*) in Niobium-Tin (Nb_3Sn). Furthermore, two *in-vessel* copper coils (*FPPC1-2*) will also be installed. Fig. 1 shows the PF coils layout of JT-60SA.

As it will be shown later, the PF coils represent the actuators used by the magnetic control system; for the sake of completeness, it is worth to mention that there exist in literature proposals to exploit the PF coils also for other control tasks (as an example in [23] the authors propose to use the in-vessel coils for burn control).

2.2. Axisymmetric control problems in tokamak

Plasma control is one of the crucial issues to be addressed in order to achieve the high performances in tokamak operations. In particular, magnetic axisymmetric control is an essential feature to achieve and maintain the desired *operational scenario*, and is needed since the very early plasma operation, including part of the integrated commissioning.

The magnetic control problem can be conceptually separated into three principal aspects [9]:

- Position control;
- Plasma current control;
- Shape control.

Position control mainly deals with the control of the plasma vertical instabilities which affect elongated plasma configurations. The task of plasma vertical stabilization is usually carried out by exploiting the in-vessel coils, which are able

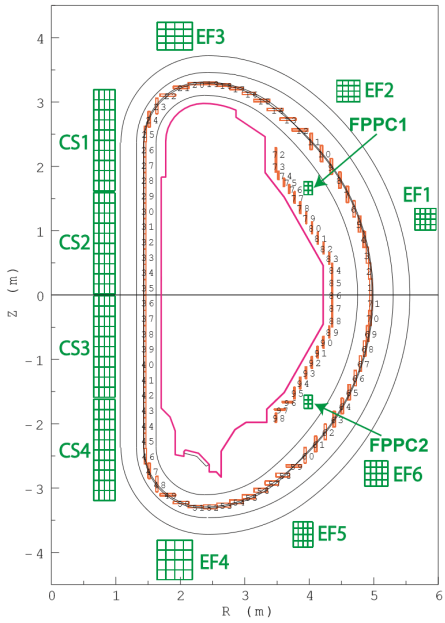

Figure 1: JT-60SA poloidal cross-section and layout of the Poloidal Field coils system.

to guarantee a faster response due to the fact that the electromagnetic field generated does not have to penetrate the metallic vessel structures. Such coils are usually made of copper in order to operate as near as possible to the hot plasma, which would make impossible to keep the superconductive coils at the requested temperatures.

In order to make the design of the other controllers straightforward and to achieve better performances, it is a good practice to design this controller with a relatively large frequency bandwidth, which translates into a fast response and a decoupling from the other control actions [14, Section III].

Plasma current control takes care of regulating the plasma current to the desired value; usually, this is done mainly (but not only) exploiting the central solenoid. The plasma, from this point of view, can be seen as the secondary coil of a transformer. Usually, it is desirable to have a plasma current control which is robust enough to work with different scenarios, independently of the desired plasma shape.

Finally, *Shape control* is responsible for the plasma to achieve a desired shape; this goal is reached by regulating the position of some points along the plasma boundary (reconstructed by a proper real-time estimation code).

It is worth to remark that, although not strictly included into the axisymmetric control problems, the regulation of the currents into the PF coils is usually included in the magnetic control system.

Indeed, plasma scenarios are defined in terms of nominal currents into the PF coils. Furthermore, the other control loops described so far can be designed in such a way to compute additional references for the PF current control. It turns out that a reliable *PF current control system* is needed, in order to track the desired references.

3. TOOLS FOR DESIGN AND VALIDATION OF MAGNETIC CONTROL

In order to design and validate the proposed architecture for the JT-60SA magnetic control system described in Section 4, a set of Matlab/Simulink® tools has been set up.

Such tools exploit linearized plasma models generated by means of the CREATE equilibrium codes. These models are integrated into a Simulink scheme which reproduces the behaviour of the magnetic control system; the simulation scheme is initialized by means of a dedicated Matlab procedure. A similar approach has already been adopted in order to reproduce the experimental behav-

ior of different fusion experimental devices, such as JET [13, 15], and more recently the EAST tokamak [2]. The availability of two different equilibrium codes, namely CREATE-L [4] and CREATE-NL [1], is exploited for code benchmarking (see Section 3.1).

The same modelling tools are currently used not only for the design of JT-60SA, but also to perform preliminary studies and code benchmarking for both ITER [22] and DEMO [32].

Both the CREATE-L and CREATE-NL equilibrium codes automatically generate linearized models which can be used to design and validate magnetic control architectures. The main differences between these two codes consist in the type of FEM elements used (respectively first and second order triangles), in the possibility of generating an inverse equilibrium (which is only possible with CREATE-L), and in the jacobian matrix calculation method for the linearization process (respectively analytical or numerical). Furthermore, CREATE-NL can be also used to validate control systems by means of nonlinear simulations, and can be also easily coupled with transport codes for integrated simulations [25].

Regardless of the specific equilibrium code used to derive it, the linearized model is given as sate-space model:

$$\delta\dot{\mathbf{x}}(t) = \mathbf{A}\delta\mathbf{x}(t) + \mathbf{B}\delta\mathbf{u}(t) + \mathbf{E}\delta\dot{\mathbf{w}}(t), \tag{1a}$$

$$\delta\mathbf{y}(t) = \mathbf{C}\ \delta\mathbf{x}(t) + \mathbf{F}\delta\mathbf{w}(t), \tag{1b}$$

where:

- **A**, **B**, **E**, **C** and **F** are the model matrices;
- $\delta\mathbf{x}(t) = \left(\delta\mathbf{I}_{PF}^{\mathrm{T}}(t)\ \delta\mathbf{I}_{eddy}^{\mathrm{T}}(t)\ \delta I_p(t)\right)^{\mathrm{T}} \in \mathbb{R}^{(n_{PF}+n_e+1)}$ is the state space vector, which includes the n_{PF}variations of the currents in the PF circuits, of the eddy currents in the n_e circuits used to model the passive structures, and the variation of the plasma current I_p;
- $\delta\mathbf{u}(t) = \left(\delta\mathbf{U}_{PF}^{\mathrm{T}}(t)\ \mathbf{0}\ U_p\right)^{\mathrm{T}} \in \mathbb{R}^{(n_{PF}+n_e+1)}$ are the input voltages variations that includes the control voltages applied to the PF circuits $\mathbf{U}_{PF}(t)$, and the opposite of the equilibrium plasma voltage, which is assumed constant and equal to $Up = -r_p I_{p_0}$, where r_p is the estimated plasma resistance, and I_{p_0} is the value of the plasma current at the equilibrium[1];

[1]Note that the eddy current circuits are shortcut.

Table 1: Comparison of the growth rate γ for two snapshots of JT-60SA Scenario 2

Equilibrium code	$t = 4.6\ s$, $I_p = 1.4\ MA$, $l_i = 0.85$, $\beta_p = 0.21$	$t = 18.6\ s$, $I_p = 5.5\ MA$, $l_i = 0.85$, $\beta_p = 0.53$
CREATE-L	8.35 s^{-1}	3.89 s^{-1}
CarMa0 2D mesh	8.32 s^{-1}	4.31 s^{-1}
CarMa0 3D mesh	9.22 s^{-1}	4.68 s^{-1}

- $\delta\mathbf{w}(t) = (\delta\beta_p(t)\ \delta l_i(t))^{\mathrm{T}} \in \mathbb{R}^2$ are the β_p and l_i variations, seen as disturbances from the magnetic control point of view;
- $\delta\mathbf{y}(t) \in \mathbb{R}^{n_y}$ is the output vector, that includes all the variables that need to be controlled (e.g., $I_p(t)$, the fluxes in the control points for plasma boundary control, the currents in the PF circuits $\mathbf{I}_{PF}(t)$, etc.).

Given the adopted description for the passive structures of JT-60SA, the order of model (1) is equal to 140.

3.1. Benchmarking of plasma equilibria

As an example of code benchmarking, this section reports on the comparison between the plasma equilibria obtained with CREATE-L, and the ones obtained with TOSCA [27] and CarMa0 [24].

In particular, Figs. 2(a) and 2(b) shows a comparison between the shape obtained with TOSCA (left-hand side) and CREATE-L (right-hand side) for Scenario 2 at $t = 4.6\ s$ and $t = 18.6\ s$, respectively.

Moreover, Table 1 reports a comparison of the growth rates obtained with both CREATE-L and CarMa0 for three snapshots of the Scenario 2. It should be noticed that the computation of the growth rate has been performed taking into account both the active coils and the passive structure, i.e. it has been assumed that the PF coils will be controlled in a *voltage-driven* mode, coherently with the proposed control architecture.

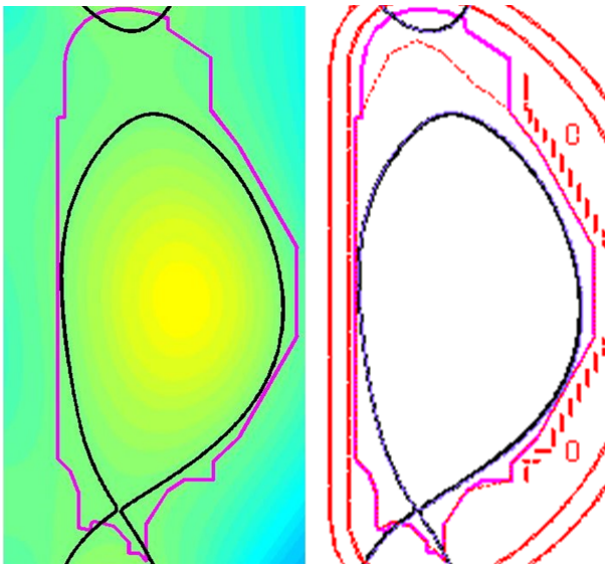

(a) Comparison for Scenario 2 at $t = 4.6\ s$.

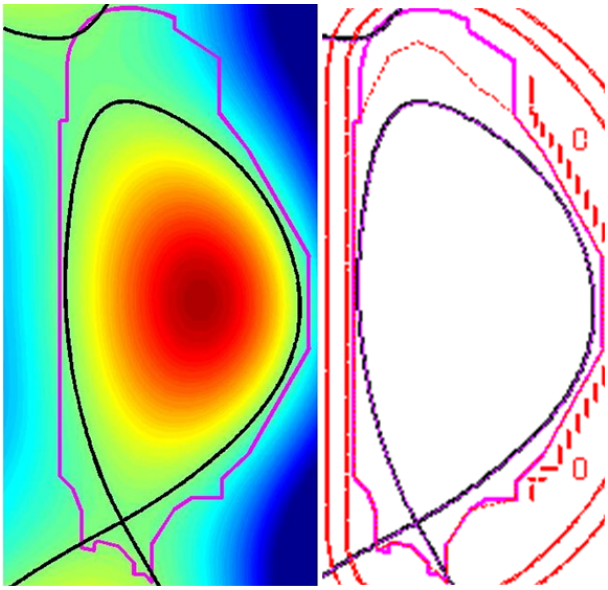

(b) Comparison for Scenario 2 at $t = 18.6\ s$.

Figure 2: Comparison of the plasma shapes obtained with the TOSCA and CREATE-L equilibrium codes for two snapshots of the JT-60SA Scenario 2.

4. PROPOSAL FOR THE JT60-SA MAGNETIC CONTROL ARCHITECTURE

In this section, a possible architecture for the JT-60SA magnetic control system is proposed and discussed. its effectiveness is shown by means of simulations, as it is reported in Section 5.

The proposed magnetic control system architecture consists of:

- A Poloidal Field Coils Current Controller, which grants that the PF coils achieve the reference current requested from the outer control loops;
- A Vertical Stabilization Controller, which takes care of vertically stabilize the unstable plasma column. For the reasons exposed in Section 2, this controller exploits the FPPC coils;
- A Plasma Current Controller, which regulates the plasma current to a desired value. This controller mainly exploits the CS coils (together with EF1-6);
- A Shape Controller, which causes the plasma boundary to move in order to achieve a desires plasma shape. This controller makes use of both EF and CS coils.

A block diagram of the control architecture is shown in Fig. 3.

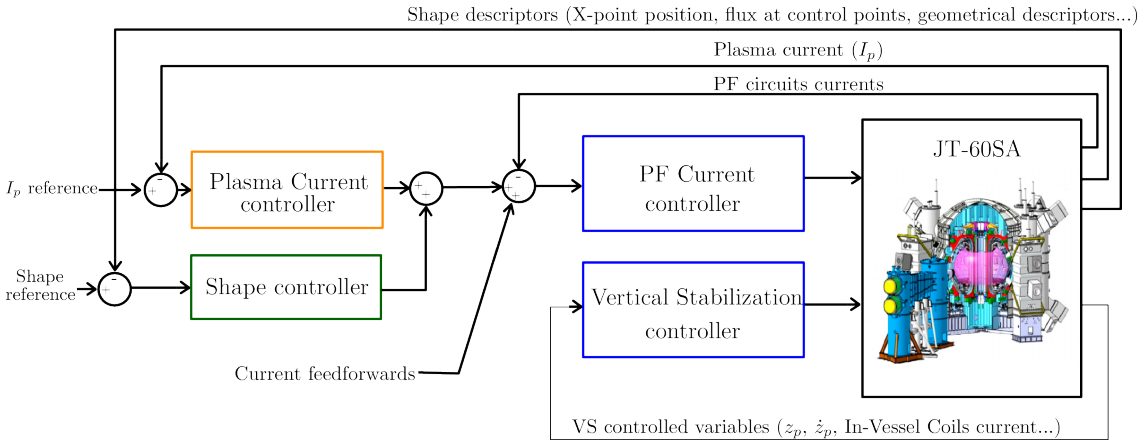

Figure 3: Proposed architecture for the JT-60SA magnetic control system.

In the following, a detailed discussion of each of the control system listed above is given.

4.1. Vertical Stabilization control

In order to vertical stabilize the plasma, two possible solutions have been explored and are presented in this section.

The first solution computes the voltage requests to the FPPC coils as a linear combination of the vertical velocity of the plasma and the FPPC *imbalance* current. Indeed, the two in-vessel coils are driven in anti-series, that is the current in the upper coil flows in the opposite way with respect to the one in the lower coil. Given this connections setup, the vertical stabilization system can consider the FPPC coils as a single circuit, where $I_{FPPC}(t)$ is the imbalance current between the two coils, and $U_{FPPC}(t)$ is the voltage to be applied, with opposite signs, to the coils.

It turns out that the voltage applied to the FPPC coils is calculated as:

$$U_{FPPC}(t) = k_1 I_{FPPC}(t) + k_2 \dot{z}_p(t)\,. \tag{2}$$

By tuning in a proper way the weights of the linear combination in (2), it is possible to obtain zero velocity in the vertical direction while maintaining low the imbalance current $I_{FPPC}(t)$ in the in-vessel coils (i.e. far from the saturation limits).

It is worth noticing that all the parameters of the controller can be kept constant when moving from one scenario to another; the only exception is the gain k_2, which scales with the inverse of the plasma current I_p.

The robustness of the proposed approach with respect to variations of the model parameters can be evaluated by means of classical single-input-single-output (SISO) tools, when the open-loop transfer function between $U_{FPPC}(t)$ and the linear combination $k_1 I_{FPPC}(t) + k_2 \dot{z}_p(t)$ is considered. As an example, the Nichols plots of the considered open-loop transfer functions obtained with linearized models of Scenario 1 at $t = 15.66\ s$, and of Scenario 2 at $t = 0.06,\ 0.16$ and $t = 18.66\ s$ are shown in Fig. 4. As it can be seen, the gain margin stays in the range $[5.58\,,\,9.83]\ dB$, while the phase margin is in the interval $[34.4\,,\,65.0]$ degrees.

It is important to remark that the simple structure of the control law (2) with just two gains, permits to foresee the realization of effective adaptive algorithms for the parameters tuning during real tokamak operations.

The second approach exploits a *near* optimal controller to achieve zero vertical position and velocity in a minimum time span. Given the system model, this method aims at simultaneously bringing the plasma to rest and to the reference position, by optimizing the time to target.

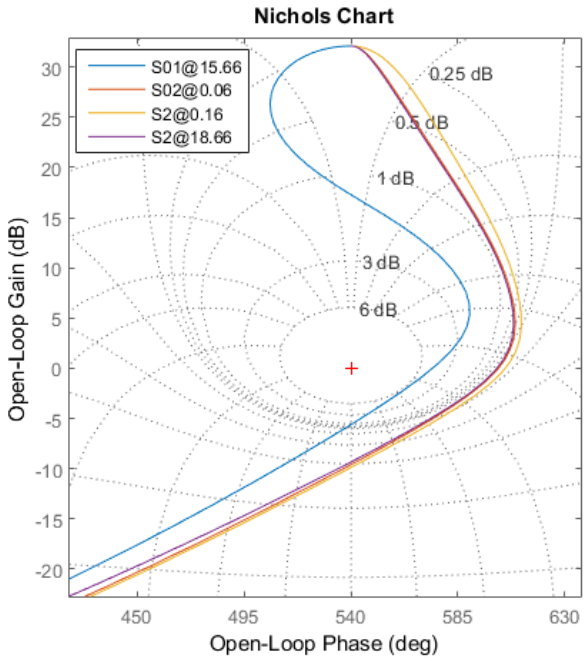

Figure 4: Nichols plots for Scenario 1 and Scenario 2.

The method applied to improve the vertical stabilization system in TCV [11, 12] was further developed using the CREATE plasma model. In [11] the method implemented for TCV Tokamak uses an extreme model reduction up to a second order model. Then this simplified model is used to build the controller. When applying the same model reduction to the JT-60SA tokamak and power supplies models, the accuracy of the reduced model was not enough to satisfy the representation of the complete model.

To solve this issue, we used a similar method to find the switch time and final time to target with the complete model, including the power supply, to design the controller. The time optimal control law algorithm using the complete model revealed to be too heavy for real-time implementation and would need the real-time input measurements of several states that are not expected to be available for control. The optimal state-space trajectory calculation needs information on the different states of the system, while the controller should only use the data from the output vector (plasma position and velocity).

To mitigate this difficulty the design of a near time optimal controller using plasma position and velocity was envisaged. The solution was to implement a PID controller with high gains tuned to approximate the behaviour of the bang-bang controller. The voltage applied to the FPPC coils is thus calculated as:

$$U_{FPPC}(t) = k_p z_p(t) + k_d \dot{z}_p(t)\,. \tag{3}$$

where $U_{FPPC}(t)$ is the previously defined voltage to be applied, with opposite signs, to the coils, while k_p and k_d are the proportional and derivative gains of the controller, and $z_p(t)$ and $\dot{z}_p(t)$ are the plasma position and velocity respectively.

4.2. Plasma Current control

The Plasma Current control problem has been solved adopting a simple PID control logic. The current references for the CS and EF coils are calculated as

$$\mathbf{I}_{PF}(s) = \mathbf{K}_{p_{curr}} \left(k_P + k_I \frac{1}{1+s\tau_I} + k_D \frac{s\tau_D}{1+s\tau_D} \right) I_{p_e}(s)\,, \tag{4}$$

where $I_{p_e}(s) = I_{p_{ref}}(s) - I_p(s)$ is the Laplace transform of the plasma current control error, while $\mathbf{K}_{p_{curr}}$ is a vector which contains a combination of the PF currents that causes a constant flux variation along a closed line containing the envisaged plasma boundary, that is is the linear combination of the PF currents that provides the so called *transformer field*. Such a combination of currents has been obtained via an optimization procedure, based on a FEM model of the machine poloidal cross section (without plasma).

Similarly to what has been seen for the vertical stabilization algorithm (2), the PID parameters in (4) can be tuned using SISO control design tools and the SISO open-loop transfer function between the considered linear combination of PF currents and I_p.

4.3. Shape control

The proposed Shape controller adopts an *Isoflux* control logic in order to achieve the desired plasma boundary: this approach aims at controlling the position of the X-point plus a set of flux differences between the flux at some control points chosen along the desired plasma boundary and the flux at the X-point itself. This purpose is obviously to be achieved by means of a proper control algorithm.

In the proposed control architecture, an *XSC-like* approach has been adopted, starting from the hypothesis that the PF current controller performs a perfect decoupling of the PF coils circuits (as discussed in Section 4.4). Under this hypothesis, each of the PF circuits can be treated as an independent SISO channels with a first order response; in particular, the time constants of the PF circuits can all be considered equal to τ_{PF}. This means that the i-th PF circuit can be modeled as:

$$I_{PF_i}(s) = \frac{I_{PF_{ref_i}}(s)}{1 + s\tau_{PF}}\,, \tag{5}$$

where $I_{PF_i}(s)$ and $I_{PF_{ref_i}}(s)$ are the Laplace transforms of the i-th PF current measurement and reference, respectively.

The XSC then controls the whole plasma shape selecting the current into the PF coils on the base of the errors on the chosen control variables. Its design is based on the linear model output equation (1b), when only the output variables $\mathbf{y}_{sh}(t) \in \mathbb{R}^{n_{sh}}$ used to control the plasma shape are considered; hence:

$$\delta\mathbf{y}_{sh}(t) = \mathbf{C}_{sh}\ \delta\mathbf{I}_{PF}(t) + \mathbf{F}_{sh}\delta\mathbf{w}(t) \tag{6}$$

Given the isoflux approach considered in this paper, the output vector $\mathbf{y}_{sh}(t)$ includes the flux differences at the control points, and the position of the X-point.

Let $\delta\mathbf{I}_{PF_N}(s)$ and $\delta\mathbf{Y}_{sh}(s)$ be the Laplace transform of the current variations in the PF coils and of the plasma shape descriptors, respectively, when neglecting the effect of the disturbances in (6), it is:

$$\delta\mathbf{Y}_{sh}(s) = \mathbf{C}_{sh}\ \delta\mathbf{I}_{PF_N}(s)\,.$$

It follows that:

$$\delta\mathbf{Y}_{sh}(s) = \frac{\mathbf{C}_{sh}}{1 + s\tau_{PF}} \cdot \delta\mathbf{I}_{PF_{ref}}(s)\,, \tag{7}$$

hence the plasma shape descriptors have the same dynamic response of the PF currents.

Moreover, from (7) it follows that the design of the plasma shape controller can be based on the $\mathbf{C}_{sh}$ matrix following the *XSC-like* approach. The interested reader can refer to [8] for more details.

Here we just recall that, since usually $n_{PF} < n_{sh}$, at steady-state it is possible to control to zero the error on n_{PF} linear combinations of plasma shape descriptors. The choice the linear combinations to be controlled is carried out minimizing the following steady-state performance index:

$$J = \lim_{t \to +\infty} (\delta \mathbf{y}_{sh_{ref}} - \delta \mathbf{y}_{sh}(t))^T (\delta \mathbf{y}_{sh_{ref}} - \delta \mathbf{y}_{sh}(t)) \,, \tag{8}$$

where $\delta \mathbf{y}_{sh_{ref}}$ are constant references to the controlled variables.

Minimization of (8) can be attained using the singular value decomposition (SVD) of the $\mathbf{C}_{sh}$ matrix. Furthermore, additional controllers can be included in the loop in order to achieve better performances during the transient. More details about how a dynamic plasma shape controller can be designed starting from the SVD of the $\mathbf{C}$ matrix can be found in [8].

Finally, it is worth notice that such a control approach can be easily adapted to control different shape descriptor such as the distance between the plasma boundary and the first wall along some desired directions (as it is done at JET [5]). The variations of such geometrical descriptors of the plasma shape are already included among the outputs of the models generated by means of CREATE-L; nevertheless, an isoflux approach has been preferred, since it is the one currently envisaged by the JT-60SA research team.

4.4. PF current control

As it has been discussed in Section 2, the controllers described in the previous sections generate references for the PF coils currents. Hence, the magnetic control system has to rely on an effective PF coils current control algorithm. Furthermore, for the design of the shape controller it is required that the PF coils are decoupled and exhibit almost the same dynamic response (see Section 4.3).

The design of the proposed PF coils current control has been carried out starting from a plasmaless model of JT-60SA, following the steps described below:

- A modified version $\widetilde{\mathbf{L}}_{PF} \in \mathbb{R}^{n_{PF}} \times \mathbb{R}^{n_{PF}}$ of the inductance matrix of the PF circuits is calculated, by neglecting the effect of the passive structures. Furthermore, in order to minimize the control effort, in each row of the $\widetilde{\mathbf{L}}_{PF}$

matrix all the mutual inductance terms which are less than the 10% of the circuit self-inductance have been neglected. Indeed, in this way the current in each circuit is controlled only by the circuits that are more coupled with it, avoiding to easily saturate the voltages without gaining any practical improvement in the control of the PF currents.

- The time constants τ_{PF_i} for the response of the i-th circuit are chosen and used to construct a matrix $\mathbf{\Lambda} \in \mathbb{R}^{n_{PF}} \times \mathbb{R}^{n_{PF}}$, defined as:

$$\mathbf{\Lambda} = \begin{pmatrix} 1/\tau_{PF1} & 0 & ... & 0 \\ 0 & 1/\tau_{PF2} & ... & 0 \\ ... & ... & ... & ... \\ 0 & 0 & ... & 1/\tau_{PF_n} \end{pmatrix} .$$

- The voltages to be applied to the PF circuits are then calculated as:

$$\mathbf{U}_{PF}(t) = \mathbf{K}_{PF} \cdot \left(I_{PF_{ref}}(t) - I_{PF}(t) \right) ,$$

where the control gain matrix $\mathbf{K}_{PF}$ is given by

$$\mathbf{K}_{PF} = \mathbf{S}^{-1} \cdot \widetilde{\mathbf{L}}_{PF} \cdot \mathbf{\Lambda} ,$$

and $\mathbf{S} \in \mathbb{R}^{n_{PF}} \times \mathbb{R}^{n_{PF}}$ is a diagonal polarity matrix that specifies the correct sign of the applied voltage for each circuit.

In the design of the PF current control, it has not been included any integral action, since the PF coils have been supposed to be perfectly superconductive (hence providing a "natural" integral action by themselves). In real operation, where this hypothesis may not be true, such a control action can be included easily; alternatively, if a good estimation of the coils resistance is available, the ohmic drop can be compensated via a feedforward action.

The bode diagrams of the closed loop PF coils current control system are reported in Fig. 5. It can be noticed how the diagonal channels (from the $i-th$ voltage to the $i-th$ current) exhibit very similar dynamic responses, while the off-diagonal channels have a much lower magnitude (hence proving that good decoupling is achieved).

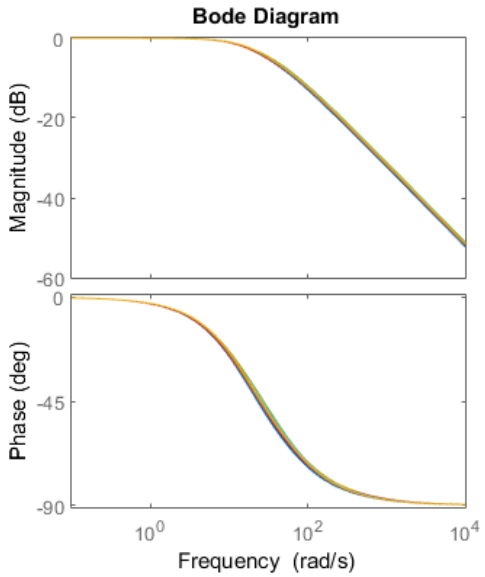

(a) Bode diagrams for the diagonal channels.

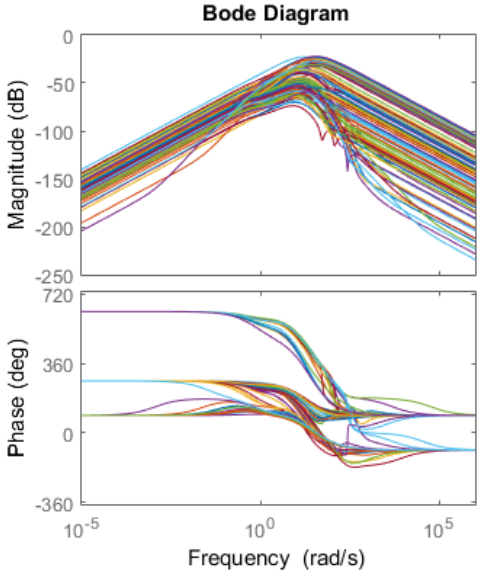

(b) Bode diagrams for the off-diagonal channels.

Figure 5: Bode diagrams for the closed loop PF coils current control system.

5. SIMULATIONS

This section shows the performance of the proposed architecture and algorithms for the magnetic control of JT-60SA. First we show the behaviour of the vertical stabilization system when the maximum possible *Vertical Displacement Event* (VDE) is considered. In the second part of this section, some preliminary simulation results of the overall magnetic control system are presented.

5.1. VDE rejection

In this section we study the performance of the near optimal vertical stabilization control system presented in Section 4.1 when rejecting a VDE. The presented results aim at evaluating the controller stability and performance, as well as assessing the controllability limits of the JT-60SA plant.

A VDE is an uncontrolled growth of the plasma unstable vertical mode. Although, the plasma is always vertically controlled, these uncontrolled growths can occur for different reasons, such as:

- fast disturbances acting on a time scale which is outside the control system bandwidth;
- delays in the control loop;
- wrong control action due to measurement noise, when plasma velocity is almost zero.

The behaviour of the near optimal vertical controller has been assessed using the linearized models of Scenarios 1 and 2. In particular, a VDE of $15\ cm$ was considered, which, for these scenarios, represent the maximum displacement that can be accommodated before the plasma touches the first wall in the outer part of the vessel. Simulations have been carried out in order to estimate how the controller and plasma would behave under this limit situation. The initial plasma velocity is calculated by the combination of states that describe the currents in the passive structures of the vessel that are calculated for the given position[2]. This makes the initial velocity a realistic worst case situation when compared to the unrealistic case of simulating initial plasma velocity and currents in the vessel as

[2]From the point of view of the vertical stabilization controller, a VDE is equivalent to a sudden and almost instantaneous change in plasma position, which causes an almost instantaneous change of the currents in model state $\mathbf{x}(t)$.

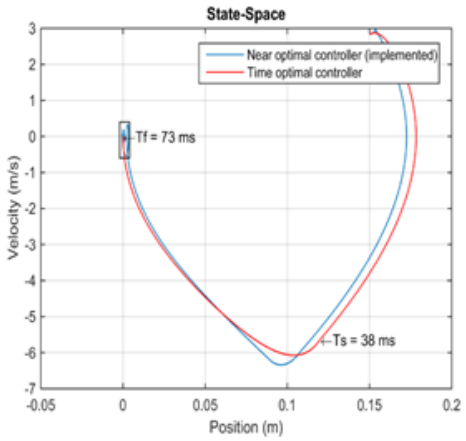

Figure 6: Time optimal and near optimal trajectories for JT-60SA Scenario 1 with initial displacement of 15 cm.

zero. Furthermore, the power supplies for the in-vessel coils have been modelled as a first order low pass filter with a time constant $\tau_{PS} = 3\ ms$, a pure delay of $1.5\ ms$, and capable to deliver a maximum voltage of $1\ kV$.

Figs. 6 and 7 present the projection of the state-space trajectory on the vertical position/vertical velocity plane when the same controller is used both for Scenario 1 and 2. The figures depict the time optimal trajectory and the near optimal trajectory that was achieved using the implemented algorithm. The same control algorithm was tested under both scenarios to check the robustness under different conditions. As a result, it turned out that the control algorithm developed for Scenario 1 was robust enough to deal also with Scenario 2.

Fig. 8 reports the time evolution of plasma position and velocity, as well as the control signal for both the optimal and the near optimal controllers in Scenario 1 case. It should be noticed that, although the near time optimal control signal has some oscillations near the set point, the overall time performance is very close to the optimal controller. The time optimal controller of the system is a bang-bang controller with a single control switch. From this example it follows that by choosing the correct gains that saturate the actuators at the given voltage limit, a PID controller can replace the bang-bang controller achieving a similar behaviour. Moreover, note that the 15 cm VDE can be recovered in less than $100\ ms$.

For the sake of completeness, Fig. 9 shows a comparison between the be-

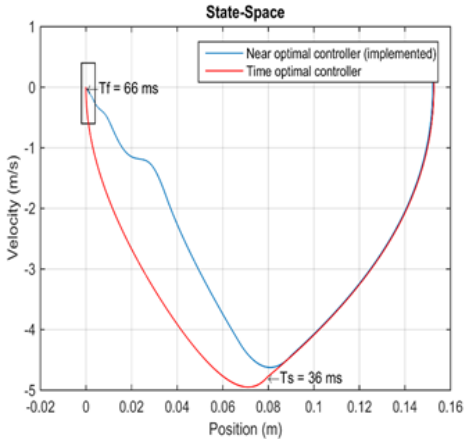

Figure 7: Time optimal and near optimal trajectories for JT-60SA Scenario 2 with initial displacement of 15 cm.

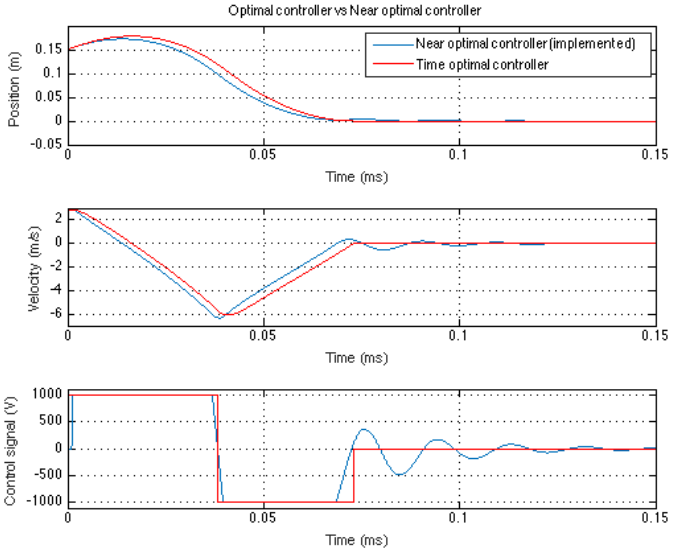

Figure 8: VDE rejection. Time evolution for the optimal and near optimal trajectories when a 15 cm VDE is considered under JT-60SA Scenario 1.

haviour of the near optimal controller and a vertical stabilization system implementing the control law (2), in the Scenario 2 case. The response of the latter is

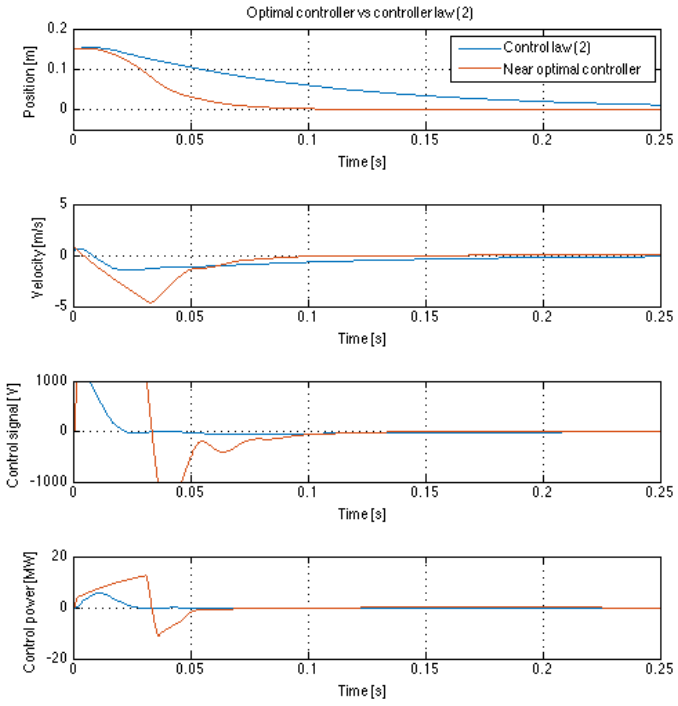

Figure 9: VDE rejection. Comparison between the near optimal controller and the control (2) when a $15\ cm$ VDE is considered under JT-60SA Scenario 2.

obviously slower (the VDE is recovered in about $150\ ms$), while the required control energy is less. Indeed, in the Scenario 2 case the control energy is about 150 kJ for the near time optimal approach, while it is about 60 kJ when (2) is applied.

5.2. Simulations of the overall magnetic control system

In this section we show the performance of the overall magnetic control system described in Section 2 by means of simulations obtained using a linearized model of Scenario 2 at $t = 0.06\ s$, which corresponds to a plasma current I_p equal to $5.5\ MA$, poloidal beta β_p equal to 0.496 and internal inductance l_i equal to 0.854.

Fig. 11 shows the Simulink scheme used to perform the simulations presented in this section. This scheme exploits the CREATE linearized model (1) and corre-

sponds to the block diagram reported in Fig 3. In this scheme a simplified model of the PF circuits power supplies has been included. Similarly to what has been done for the in-vessel coils, each power supply has been modelled as a first order system with a $3\ ms$ time constant, a pure delay of $1.5\ ms$, and a voltage saturation.

It is worth to notice that, in the current version the CREATE linearized model provides all the reconstructed parameters as outputs[3]. However, by exploiting Simulink modularity, in future a block that models the plant magnetic diagnostic can be easily included in order to take into account the nonlinearities due to the reconstruction when validating the control algorithms (as it has been done in the case of the JET tokamak, see [13]).

The results shown in Figs. 12 - 15, correspond a I_p variation of -0.5 MA in $5\ s$, plus a modification of the shape as shown in Fig. 10. The final shape is the one obtained generating a plasma equilibrium with CREATE-L for Scenario 2 at $t = 116.4\ s$; this equilibrium has been used also to obtain the final values of β_{pol} and l_i; for the simulation purposes, the disturbances ramp from the initial to the final value during the transition time.

CONCLUSION

This paper reported on the European activities carried out for the design and validation of the JT-60SA magnetic control system. In particular a proposal for the overall architecture of the plasma magnetic control system has been presented, together with the algorithms to be implemented in each functional block. Validation of the proposed approach has been proved by means of simulations, that exploits the CREATE plasma models and the simplified models of the power supplies (that includes also voltage and current saturations). In future, the modularity of the presented tools, which are based on Matlab/Simulink®, permits to easily include more detailed models of the plant (i.e., of the plasma/circuit model and/or the power supplies and/or the real-time plasma reconstruction code) in order to perform further validation of the control system.

Eventually, it is worth to remark that, by exploiting the experience previously gained on a large number of fusion devices, the CREATE modeling tools have

[3] All the quantities of interest for plasma magnetic control, i.e. the plasma current, the plasma shape and position, are reconstructed from the measurements delivered by the magnetic diagnostic system [17].

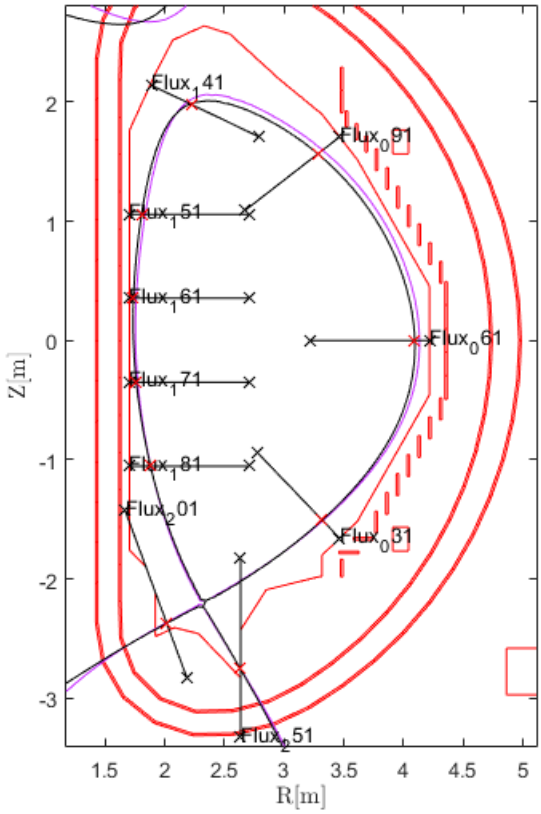

Figure 10: Shape references for the simulation. The initial shape is shown in magenta, the target shape in black; the red markers represent the target points along the control segments.

been easily customized for JT-60SA, allowing to design and validate an effective architecture for the complete magnetic control system.

ACKNOWLEDGEMENTS

The authors gratefully acknowledge members of JT-60SA Integrated Project Team for data exchange and fruitful discussions.

This work has been carried out within the framework of the EUROfusion Consortium and has received funding from the Euratom research and training pro-

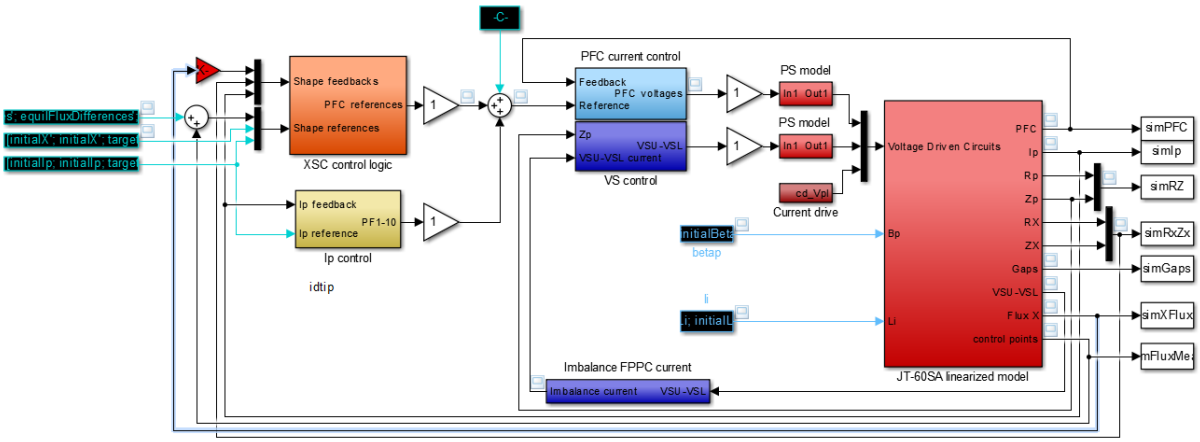

Figure 11: Simulink scheme for the JT-60SA magnetic control system.

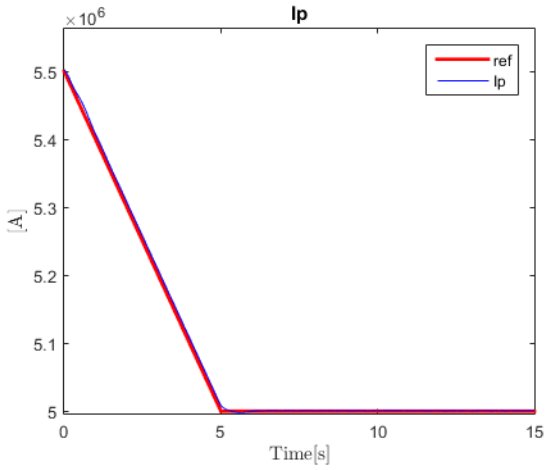

Figure 12: Plasma current.

gramme 2014-2018 under grant agreement No 633053.

IST activities also received financial support from “Fundação para a Ciência e Tecnologia” through project UID/FIS/50010/2013.

The views and opinions expressed herein do not necessarily reflect those of the European Commission.

[1] R. Albanese, R. Ambrosino, and M. Mattei. CREATE-NL+: A robust

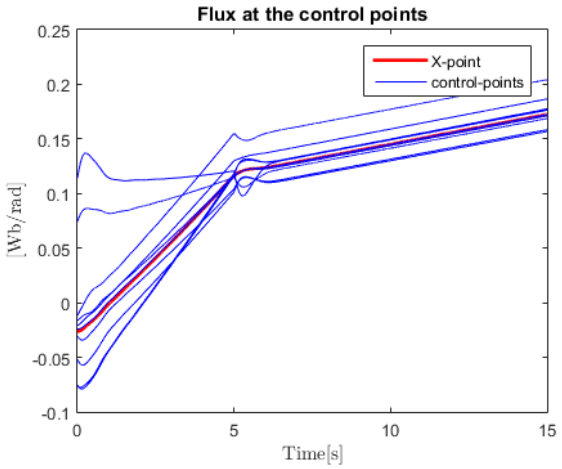

Figure 13: Fluxes at the control point.

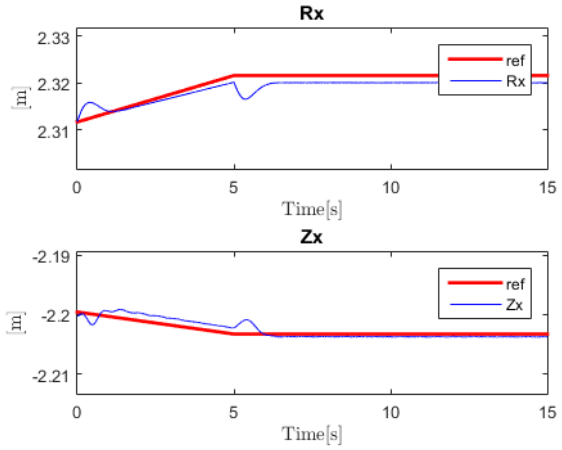

Figure 14: Position of the X-point; the small bump at 5 second is due to the artificial waveforms assigned to poloidal beta and internal inductance.

control-oriented free boundary dynamic plasma equilibrium solver. *Fus. Eng. Des.*, 96–97:664–667, Oct. 2015.

[2] R. Albanese et al. A MIMO architecture for integrated control of plasma shape and flux expansion for the EAST tokamak. In *Proc. of the 2016 IEEE*

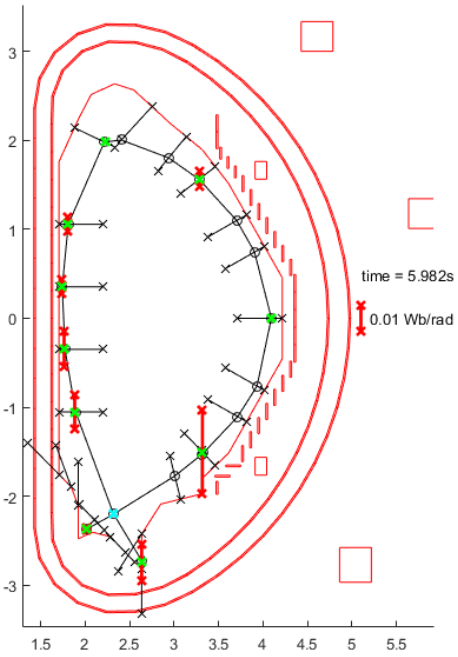

(a) Plasma shape at $t = 6\ s$.

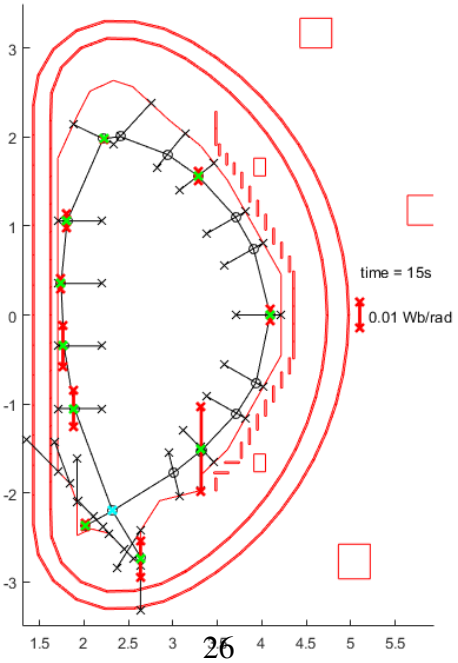

(b) Plasma shape at $t = 15\ s$

Figure 15: Snapshots of the plasma poloidal cross section during the simulation.

Multi-Conf. Syst. Contr., pages 611–616, Buenos Aires, Argentina, September 2016.

[3] R. Albanese, M. Mattei, and F. Villone. Prediction of the growth rates of VDEs in JET. *Nucl. Fus.*, 44(9):999–1007, Sep. 2004.

[4] R. Albanese and F. Villone. The linearized CREATE-L plasma response model for the control of current, position and shape in tokamaks. *Nucl. Fus.*, 38(5):723–738, May 1998.

[5] G. Ambrosino, M. Ariola, A. Pironti, and F. Sartori. Design and Implementation of an Output Regulation Controller for the JET Tokamak. *IEEE Trans. Control Syst. Technol.*, 16(6):1101–1111, Nov. 2008.

[6] R. Ambrosino et al. Design and nonlinear validation of the ITER magnetic control system. In *Proc. of the 2015 IEEE Multi-Conf. Syst. Contr.*, pages 1290–1295, Sydney, Australia, September 2015.

[7] M. Ariola, G. Ambrosino, A. Pironti, J. B. Lister, and P. Vyas. Design and experimental testing of a robust multivariable controller on a tokamak. *IEEE Trans. Control Syst. Technol.*, 10(5):646–653, Sep. 2002.

[8] M. Ariola and A. Pironti. The design of the eXtreme Shape Controller for the JET tokamak. *IEEE Control Sys. Mag.*, 25(5):65–75, Oct. 2005.

[9] M. Ariola and A. Pironti. *Magnetic Control of Tokamak Plasmas*. Springer, 2^{nd} edition, 2016.

[10] S. L. Chen et al. Equivalent axisymmetric plasma response models of EAST. *Plasma Phys. Control. Fusion*, 58(2):025017–7, Feb. 2016.

[11] N. Cruz et al. An optimal real-time controller for vertical plasma stabilization. *IEEE Trans. Nucl. Science*, 62(6):3126–3133, Dec. 2015.

[12] Nuno Cruz. *Digital Control System for Vertical Stability of the TCV Plasma*. PhD thesis, 2014.

[13] G. De Tommasi et al. XSC Tools: a software suite for tokamak plasma shape control design and validation. *IEEE Trans. Plasma Sci.*, 35(3):709–723, Jun. 2007.

[14] G. De Tommasi et al. Current, position, and shape control in tokamaks. *Fusion Sci. Technol.*, 59(3):486–498, Apr. 2011.

[15] G. De Tommasi et al. A Software Tool for the Design of the Current Limit Avoidance System at the JET Tokamak. *IEEE Trans. Plasma Sci.*, 40(8):2056–2064, Aug. 2012.

[16] G. De Tommasi et al. Shape control with the eXtreme Shape Controller during plasma current ramp-up and ramp-down at JET tokamak. *J. Fusion Energ.*, 33(2):233–242, Mar. 2014.

[17] G. De Tommasi, A. C. Neto, A. Pironti, and C. Sterle. Optimal allocation of the diagnostic signals for the ITER magnetic control system. In *Proc. of the 2015 IEEE Multi-Conf. Syst. Contr.*, pages 1296–1302, Sydney, Australia, September 2015.

[18] G. Giruzzi et al. Physics and operation oriented activities in preparation of the JT-60SA tokamak exploitation. In *Proc. of the* 26^{th} *IAEA Fusion Energy Conf.*, Kyoto, Japan, October 2016.

[19] P. Innocente et al. Requirements for tokamak remote operation: Application to JT-60SA. *Fus. Eng. Des.*, 96–97:799–802, 2015.

[20] JT-60SA Research Unit. JT-60SA Research Plan - Research Objectives and Strategy. Technical report. http://www.jt60sa.org/pdfs/JT-60SA_Res_Plan.pdf.

[21] Y. Miyata, T. Suzuki, S. Ide, and H. Urano. Study of Plasma Equilibrium Control for JT-60SA using MECS. *Plasma and Fus. Res.*, 9:3403045–5, 2014.

[22] A. C. Neto et al. Conceptual architecture of the plant system controller for the magnetics diagnostic of the ITER tokamak. *Fus. Eng. Des.*, 96–97:887–890, Oct. 2015.

[23] A. Pajares and E. Schuster. Nonlinear Burn Control in Tokamaks using In-Vessel Coils. In *Proc. of the 2016 IEEE Multi-Conf. Syst. Contr.*, pages 617–622, Buenos Aires, Argentina, September 2016.

[24] A. Portone et al. Linearly perturbed MHD equilibria and 3D eddy current coupling via the control surface method. *Plasma Phys. Control. Fusion*, 50(8):085004–12, Aug. 2008.

[25] M. Romanelli et al. JINTRAC: A System of Codes for Integrated Simulation of Tokamak Scenarios. *Plasma and Fus. Res.*, 9(special issue 2):3403023–1–4, 2014.

[26] F. Sartori, G. De Tommasi, and F. Piccolo. The Joint European Torus. *IEEE Control Sys. Mag.*, 26(2):64–78, Apr. 2006.

[27] K. Shinya. Equilibrium Analysis of Tokamak Plasma. *J. Plasma and Fus. Res.*, 76(5):479–488, May 2000.

[28] H. Shirai, P. Barabarschi, and Y. Kamada. Progress of JT-60SA Project: EU-JA joint efforts for assembly and fabrication of superconducting tokamak facilities and its research planning. *Fus. Eng. Des.*, 2016. In press.

[29] T. Tsunematsu. Broader Approach to fusion energy. *Fus. Eng. Des.*, 84:122–124, 2009.

[30] F. Villone, P. Vyas, J. B. Lister, and R. Albanese. Comparison of the CREATE-L plasma response model with TCV limited discharges. *Nucl. Fus.*, 37(10):1395–1410, Oct. 1997.

[31] W. R. Spears. JT-60SA Construction Status. *IEEE Trans. Plasma Sci.*, 42:427–431, Mar. 2014.

[32] R. Wenninger et al. Advances in the physics basis for the European DEMO design. *Nucl. Fus.*, 55(6):063003–7, Jun. 2015.

[33] Q. P. Yuan et al. Plasma current, position and shape feedback control on EAST. *Nucl. Fus.*, 53(4):043009, Apr. 2013.

[34] L. Zabeo et al. Overview of magnetic control in ITER. *Fus. Eng. Des.*, 89(5):553–557, May 2014.